Supporting Information

Effects of nanostructuration on the electrochemical performance of metallic bioelectrodes

Sahba Mobini[*], *María Ujué González, Olga Caballero-Calero, Erin E. Patrick, Marisol Martín-González, José Miguel García-Martín*

Instituto de Micro y Nanotecnología, IMN-CNM, CSIC (CEI UAM+CSIC), Isaac Newton 8, E-28760, Tres Cantos, Madrid, Spain

Department of Electrical and Computer Engineering, University of Florida, Center Drive 968, Gainesville, FL 32603, USA

† These authors contributed equally to this work.

a. Fabrication

Figure S1 shows a sketch of the fabrication method and the associated parameters.

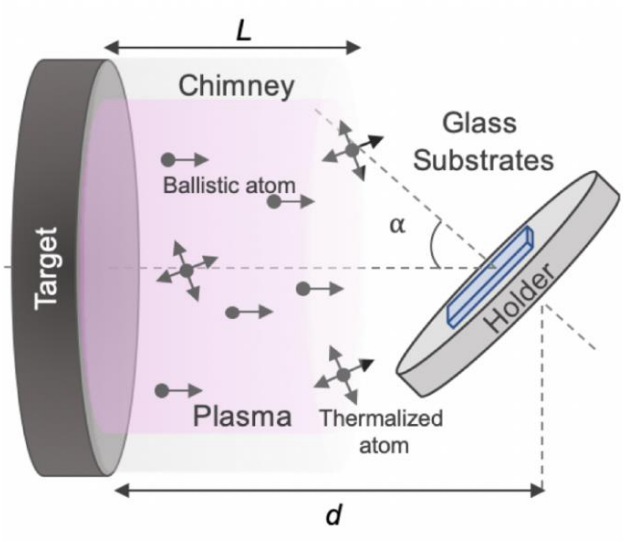

Figure S1. Schematic diagram of the fabrication method, adapted from Ref. [1].

b. RAAT Setup

We adapted the reactive accelerated aging test (RAAT) from the procedure developed by Takmakov *et al.*[2] The details of this setup are shown in **Figure S2**.

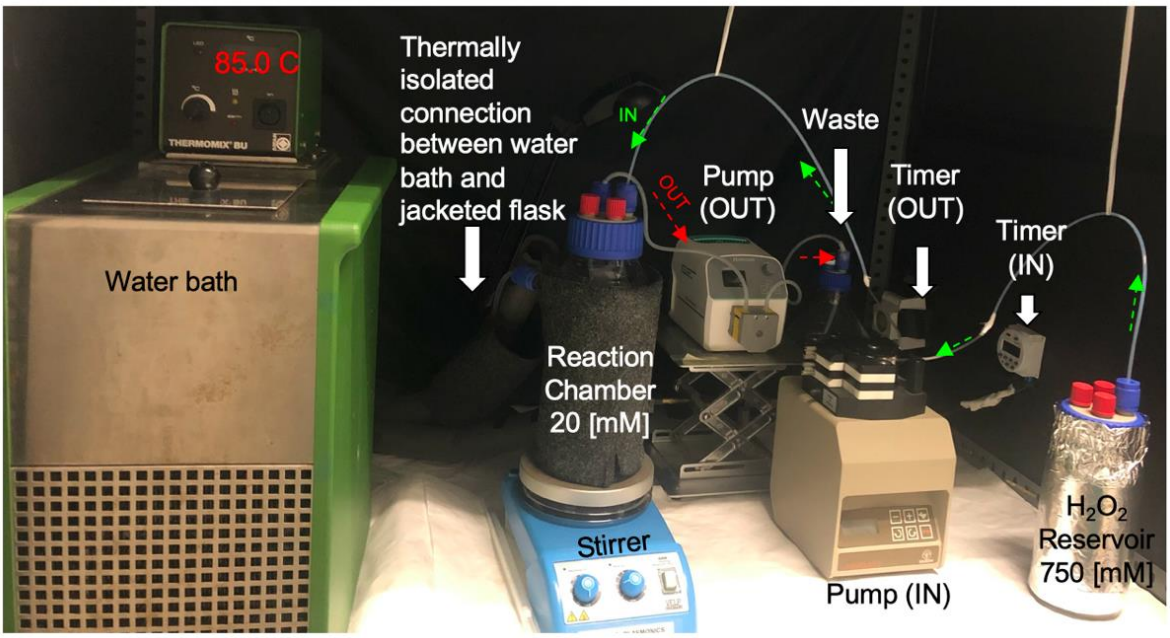

Figure S2. Reactive accelerated aging test (RAAT) setup.

Oxygen peroxide decays to half the concentration in 96 min at 85ºC, as it can be seen in Figure S3.

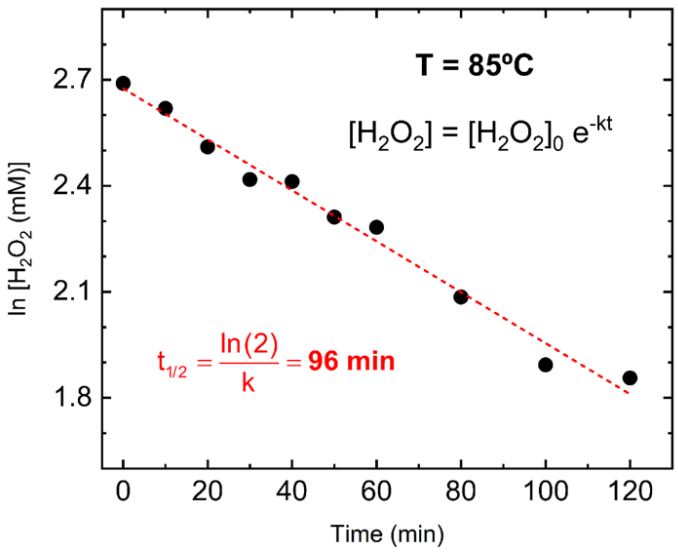

Figure S3. H_2O_2 half-life time at 85ºC.

The MATLAB code used to calculate the cycles for H_2O_2 introduction to keep the concentration between 10 and 20 mM can be found below.

MATLAB Code:

```
%Program to follow the dynamics of the AAR setup as a
%function of time
%Instituto de Micro y Nanotecnología, IMN-CNM (CSIC)

clear; clc;

%Experimental setup conditions
label_g = 'H2O2 concentration evolution simulation'; % Title of the graph (experiment name)
Tl =90; %half-life time, min
k = log(2)/Tl;
Tin = 15; %Input  cycles, min
Tout = 240; %Suction cycles, min
Vini = 750; %Initial volumne, ml
TTd =3; %Total time, days
TTm = TTd * 24 * 60;

R=Tout/Tin; %Ratio time in/out
%dimension C(R)
S=TTm/Tout; %Ratio total time / time out
%dimension CC(S)
%dimension time (Tin*R*S)

Cini = 20; %Initial concentration (mM)
Cres = 750; %Reservoir conentration (mM)
Vin = 2.3; %Input volume (ml)
Vout = Vin*R; %=38 %Suction volume (ml)
%Ideally, Vout = Vin*R

%Loop for concentration evolution in several output cycles
CC0 = Cini;
VV0 = Vini;
```

```
TT0 = 0;
for j=1:S
%Concentration evolution in an only input cycle
   C0 = CC0;
   V0 = VV0;
   T0 = TT0;
   for i=1:R
      for time = 0:Tin
         tplot ((j-1) * Tin * R + (i-1)*Tin + time + 1) = time + T0;
         Cplot ((j-1)* Tin * R + (i-1)*Tin + time + 1) = C0 * exp(-k*time);
      end
      Cend = C0 * exp(-k*Tin); %Concentration after Tin cycle, following 1st order dynamics
      C(i)= (Cres*Vin + Cend*V0)/(V0 + Vin);
      C0 = C(i);
      V0 = V0 + Vin;
      T0 = T0 + Tin;
   end
   VV0 = V0-Vout;
   CC0 = C0;
   TT0 = T0;
end
figure(1);
plot(tplot/60,Cplot,'b');
title (label_g);
ylabel ('Concentration (mM)');
xlabel('Time (hours)');
hold on;

Cfinal = CC0;
```

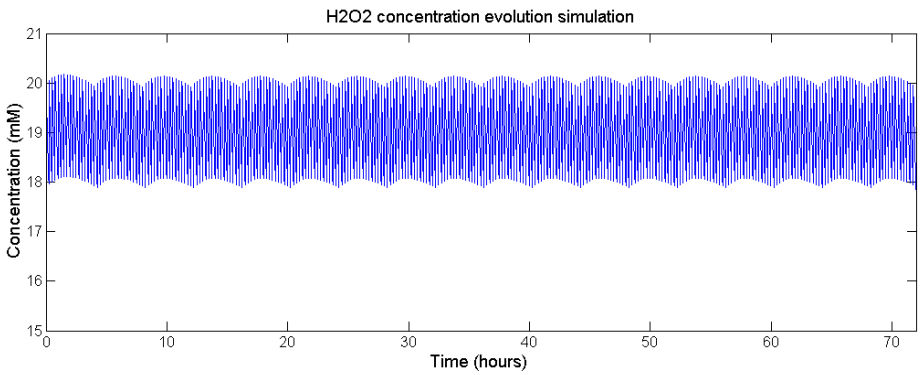

c. Electrochemical characterization

The electrochemical characterization has been performed in a chamber (10 mm × 10 mm × 10 mm) with fix amount of electrolyte. The working electrode and platinum mesh (counter electrode) were secured at a distance of 10 mm and 300 µl of PBS (electrolyte) were used for each experiment to assure a reproducible electrode immersion height of 3 mm. The setup is shown in Figure S4.

Figure S4. Electrochemical characterization setup.

All electrochemical characterizations described in the main text has been performed on several replicates (at least 3 independent samples, 2 measurements). The average $Z \pm$ SD and individual data points for all metals (Ti, Au, Pt) and morphologies at frequencies of 1, 40, and 1000 Hz are shown in **Figure S5**.

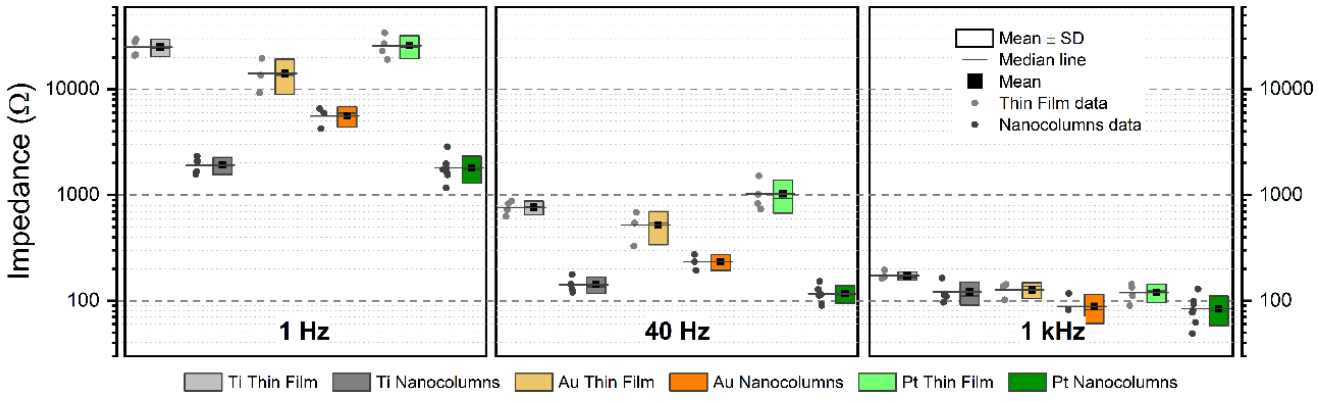

Figure S5. Average impedance at 1, 40 and 1000 Hz.

The electrochemically active surface area (ECSA) of each morphology and material was determined using cyclic voltammetry with different sweep rates, as explained in the main text. Figure S6 shows the I vs. dE/dt (sweep rate) plots. The slope of the plots (I vs. dE/dt) provides the double layer capacitance for each system.

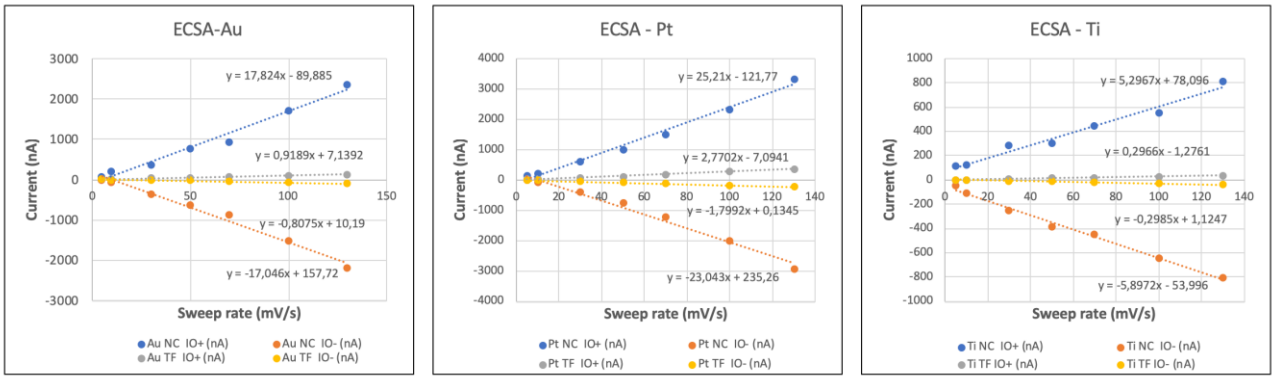

Figure S6. I vs. dE/dt (sweep rate) plots for each metal NCs and TFs.

d. Morphology

Roughness and nanostructure of metallic surfaces play important role in electrochemical performance. Surface interrogation techniques such as Atomic Force Microscopy (AFM) are generally used to calculate roughness. Root mean square of surface (RMS) is one of the indicators for expressing roughness. Figure S7 presents the AFM images of the different textures and materials analyzed.

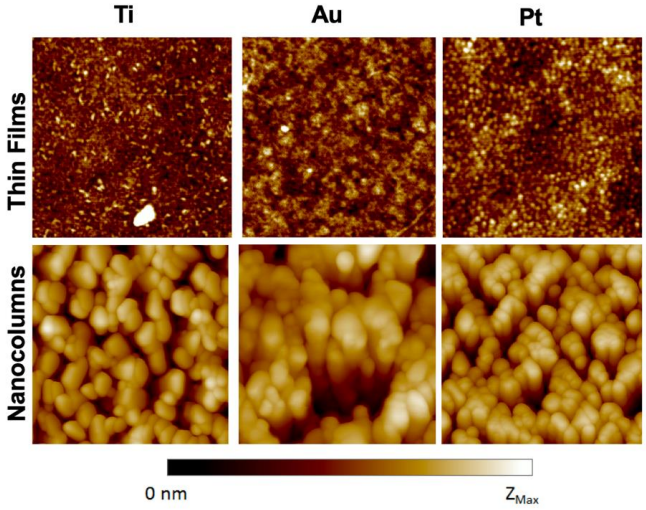

Figure S7. AFM images (size: 1 × 1 μm^2), the maximum height Z_{Max} of the color scale has been adjusted in each case to improve the final output. Ti TF, Z_{Max} = 3 nm; Au TF, Z_{Max} = 3.5 nm; Pt TF, Z_{Max} = 2.3 nm; Ti NCs, Z_{Max} = 194 nm; Au NCs, Z_{Max} = 222 nm; Pt NCs, Z_{Max} = 147 nm.

However, as explained in the main text, there are several artifacts associated with this measurement in result of the limitation of penetration of the tip down to the substrate in every inter-columnar space due to the high aspect ratio of NC features. Nonetheless, we made a measurement to have an estimate of such roughness. Results are shown in **Table S1**. RMS of the samples was obtained as the average from the values calculated in four different images in 1 × 1 μm^2 and 2 × 2 μm^2 scanned areas.

Table S1. RMS roughness (nm) of the samples.

	Ti	Au	Pt
NCs	29.7 ± 0.5	33.6 ± 1.8	21.8 ± 0.5
TF	0.7 ± 0.1	0.5 ± 0.1	0.3 ± 0.1

e. Simulation

We demonstrate the result of a transient electrical simulation for NCs compared to TFs. Results for the Pt NCs are demonstrated in the main text as an example. Ti and Au showed a trend similar to Pt, **Figure S8**. NCs in general demonstrate less filtering effect on applied voltage (V_{App}) and consequently less attenuation in delivered signal in the medium (V_{Re}) compared to TFs.

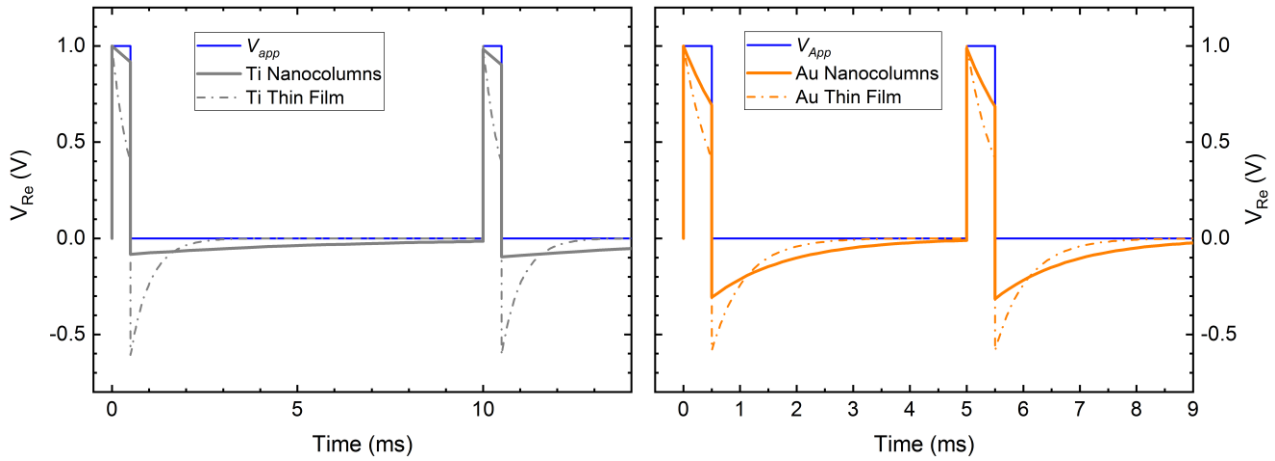

Figure S8. Simulation of Ti and Au NCs and TFs in voltage-controlled system shows TFs has greater filtering effect on the applied signal compared to NCs.

f. Effect of Reactive Accelerated Aging Test

f.1. Aging of Ti

Aging of Ti causes TiO_2 formation due to acute oxidation. This consequently gives rise to delamination of Ti NCs and partial delamination of Ti TFs and formation of pits and holes on the surface. We measured a significant increase in the amount of anatase on the surface by means of Raman spectroscopy, **Figure S9.** The peak that appears at 137.7 cm^{-1} indicates the presence of anatase.[3] This peak is larger in the case of aged Ti TF, which confirms formation of the oxide on the surface that consequently causes delamination and pit formation.

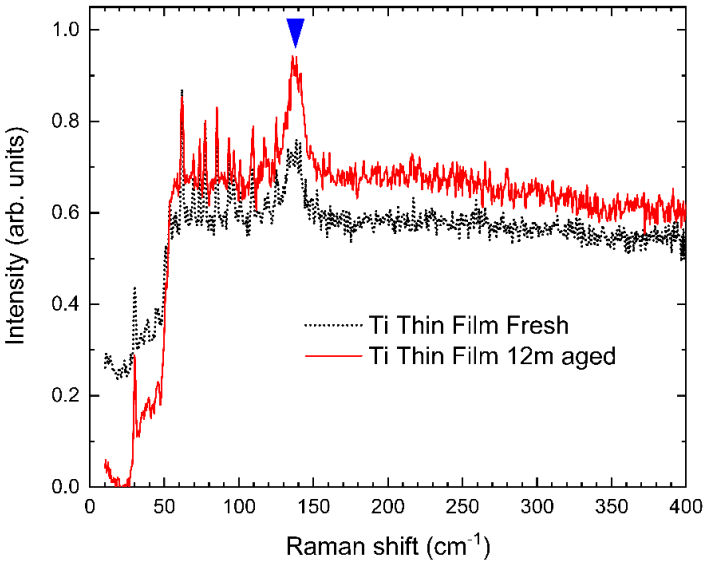

Figure S9. Raman spectra for Ti TFs before and after aging.

Another interesting observation on Ti TF aging compared to Pt and Au is the amount of NaCl precipitate found on the surface of these samples. **Figure S10** presents the elemental mapping obtained by EDX, which shows the existence of Cl on the surface of aged Ti TF. Considering that Na is an abundant element in the composition of the glass substrate, we used Cl as a proof for existence of NaCl, since its only source is the NaCl of the PBS. We also found plenty amount of oxygen coexisting with Ti, as another proof for presence of TiO_x.

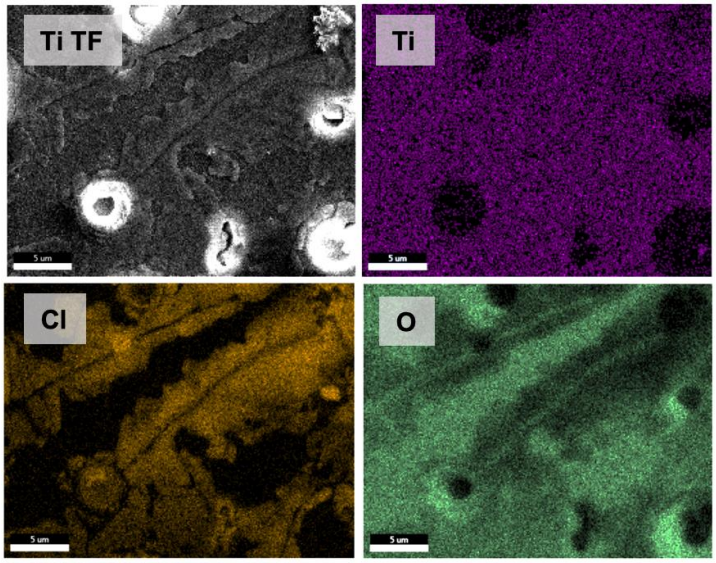

Figure S10. EDX map of elements (Ti, O, Cl) for aged Ti TFs. Scale bar = 5 μm.

f.2. Aging of Au

Interestingly, Au was the element that was changed the least after aging. We found almost no precipitate of NaCl on Au TFs and NCs. However, in SEM images we observed that the grains size of the Au TF and NCs (less evident) has been increased after aging. Due to low melting temperature, the grains expand when treated at 85 °C. The results are shown in **Figure S11**.

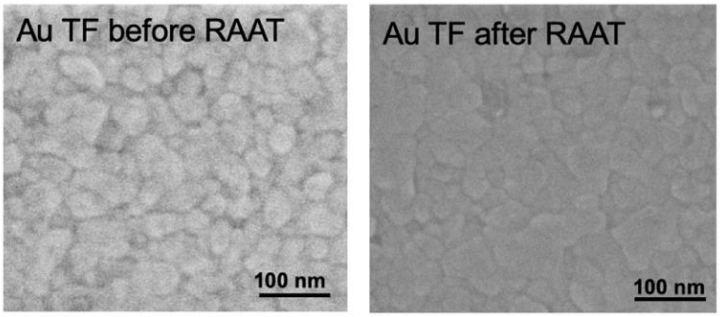

Figure S11. SEM images of Au TF before and after RAAT shows slight increase of the grain size.

This could be the reason for the slight change in the electrochemical properties and equivalent circuit after aging. Here we showed differences in the equivalent circuit extracted from *Nyquist plots of* Au TFs and NCs before and after again, **Table S2**. To use more representative symbols, R_s is mentioned in the main text as R_e (resistivity of the electrolyte) and R_p is mentioned as R_f (resistivity of the faradaic charge injection).

Table S2. Equivalent circuits.

Sample	Before Aging	After Aging
Au TF	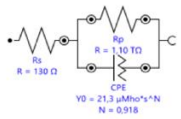	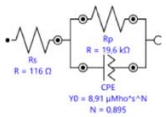
Au NCs	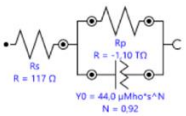	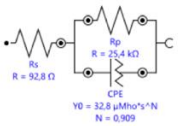

The EDX elemental mapping of Au NCs, **Figure S12**, reveals that there is almost no NaCl precipitate on the surface and no composition change in Au NCs after RAAT.

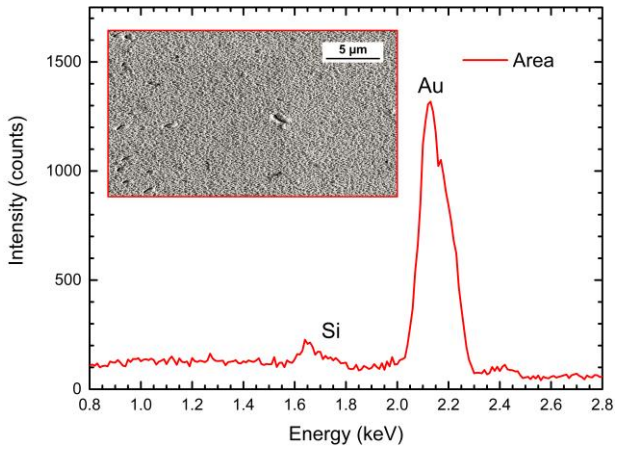

Figure S12. EDX element analysis for Au NCs after RAAT.

f.3. Aging of Pt

We found NaCl precipitates on Pt TF and Pt NCs after aging. The amount deposited on Pt was less than on Ti TF but still noticeable. Here we demonstrate this with representative EDX elemental mapping image, **Figure S13** and **S14**. The EDX spectrum for Pt NCs is shown in **Figure S15**.

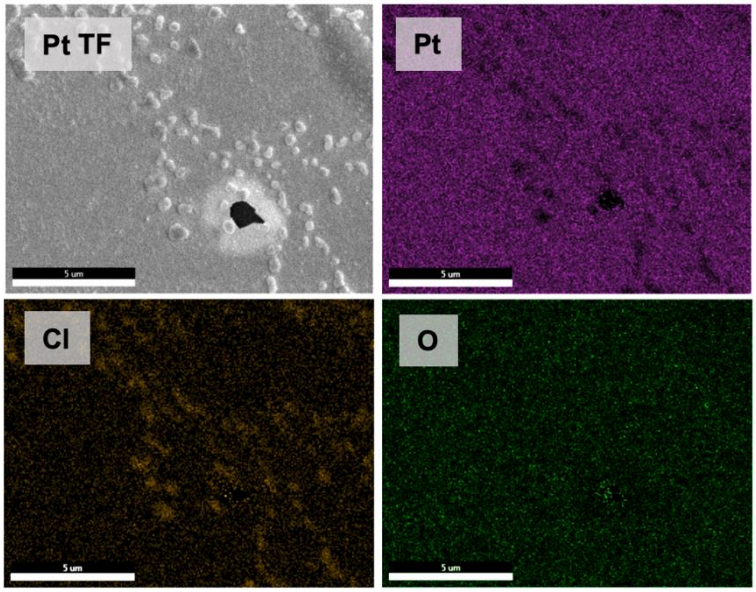

Figure S13. EDX map of elements (Pt, O, Cl) for aged Pt TFs. Scale bar = 5 μm

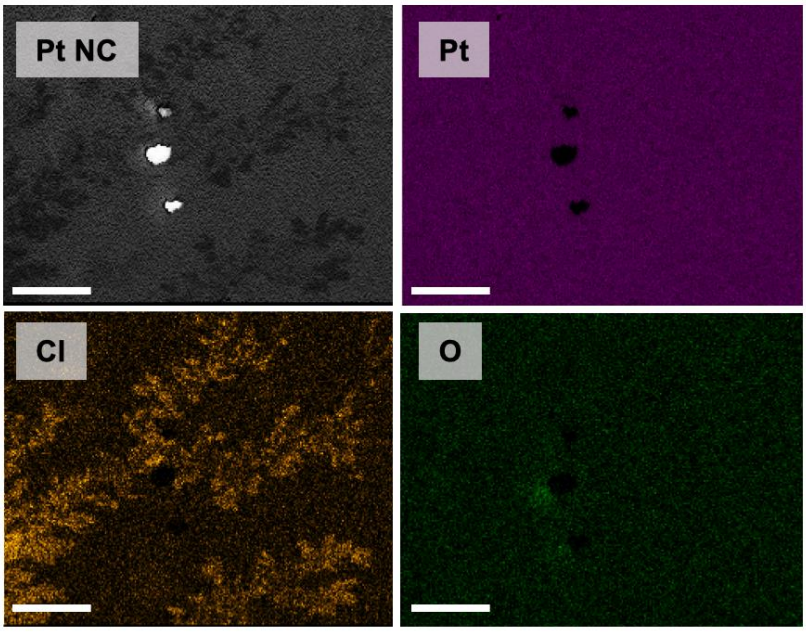

Figure S14. EDX map of elements (Pt, O, Cl) for aged Pt NCs. Scale bar = 5 μm

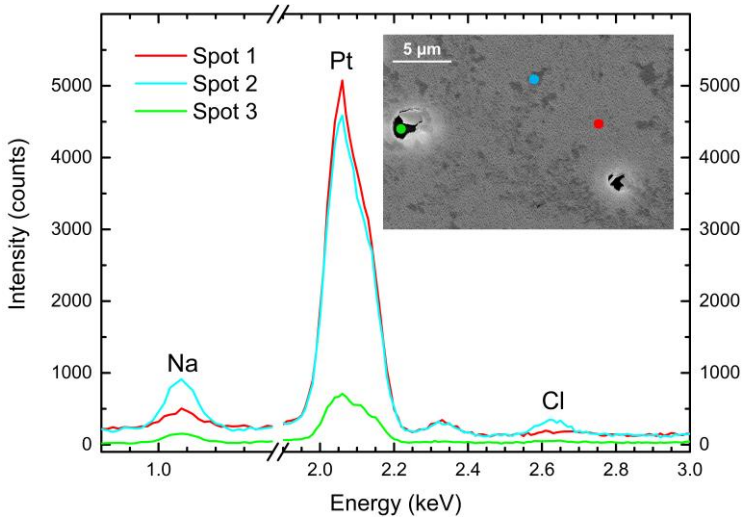

Figure S15. EDX element analysis for Au NCs after RAA.

REFERENCES

[1] R. Alvarez, J. M. Garcia-Martin, M. C. Lopez-Santos, V. Rico, F. J. Ferrer, J. Cotrino, A. R. Gonzalez-Elipe and A. Palmero, Plasma Process. Polym., 2014, **11**, 571–576.

[2] P. Takmakov, K. Ruda, K. Scott Phillips, I. S. Isayeva, V. Krauthamer and C. G. Welle, J. Neural Eng., 2015, **12**, 026003.

[3] O. Frank, M. Zukalova, B. Laskova, J. Kürti, J. Koltai and L. Kavan, Phys. Chem. Chem. Phys., 2012, **14**, 14567–14572.